

Cite this article as: Zou Juntao, Song Dazhuo, Lei Yi, et al. Effects of Sandblasting and Annealing on Surface Recrystallization of DD483 Superalloy[J]. Rare Metal Materials and Engineering, 2022, 51(01): 106-112.

ARTICLE

Effects of Sandblasting and Annealing on Surface Recrystallization of DD483 Superalloy

Zou Juntao¹, Song Dazhuo¹, Lei Yi^{1,2}, Zhuo Longchao¹, Shang Zhao¹, Yang Gongxian², Zhang Qiongyuan², Gong Xiufang²

¹Engineering Research Center of the Ministry of Education for Conductive Materials and Composite Technology, Xi'an University of Technology, Xi'an 710048, China; ²State Key Laboratory of Long-Life High Temperature Materials, Dong Fang Turbine Co., Ltd, Deyang 618000, China

Abstract: The microstructure evolution and surface recrystallization behavior of sandblasted DD483 Ni-based superalloys after heat treatment around the service temperature were investigated. The specimens of DD483 alloy were sandblasted under the pressure of 0.4~0.7 MPa and annealed at 1100 °C for 4 and 16 h. The results show that the surface of the alloy is effectively cleaned and the compressive stress is introduced into the surface by sandblasting within the range of predetermined sandblasting pressure. After annealing for 4 and 16 h, the Ti and Al elements volatilize to the surface in the form of oxides, and the cellular recrystallization structure appears on the specimen subsurface. The topologically close-packed (TCP) phase and TiN are precipitated in the recrystallized region and the original matrix near recrystallized region, respectively. In addition, the thickness of the recrystallized region is increased with increasing the annealing time and the actual stress.

Key words: Ni-based superalloys; sandblasting; annealing; recrystallization; surface; microstructure

Directionally solidified superalloys are widely used in the manufacture of turbine blades for aero-engines and gas turbines due to their excellent high-temperature mechanical properties^[1,2]. The directional solidification process can eliminate the lateral grain boundaries which are perpendicular to the stress axis, and this process can effectively prevent the crack initiation and propagation^[3]. However, the blades often suffer a certain plastic deformation on the surface, such as shrinkage, bumping, sandblasting, and machining^[4,5], resulting in the surface recrystallization during high-temperature service. Among them, sandblasting is used to remove mold debris from cast components as well as to prepare the bond coat surface prior to deposition of thermal barrier coatings (TBCs), which is indispensable for preparing blades^[6]. The recrystallization of directionally solidified superalloys caused by strain and residual stress is a key problem in the investment casting industry^[7]. It is generally believed that a certain

volume of recrystallization can significantly reduce the creep rupture strength and fatigue life of superalloys^[8]. Much effort has been made to understand the recrystallization behavior of directionally solidified single crystal superalloys^[9-11], but the surface recrystallization of directionally solidified DD483 alloy after sandblasting and subsequent heat treatment is rarely investigated. Therefore, it is necessary to study and control the surface recrystallization of DD483 alloy.

In this research, the microstructure evolution and surface recrystallization behavior of sandblasted DD483 alloy after heat treatment around the service temperature were investigated. The relationships among the sandblasting pressure, residual stress, and the microstructural instability zone on surface were investigated, providing a foundation for controlling the surface recrystallization of the directionally solidified superalloys.

Received date: January 27, 2021

Foundation item: National Natural Science Foundation of China (52071259, 51834009); National Key R&D Program of China (2017YFE0301402); Research Program of Science and Technology of Shaanxi Province (2020zdzx04-04-01, 2018ZDXM-GY-136, 20JY050); Sponsored by State Key Laboratory of Long-Life High Temperature Materials (DTCC28EE190226)

Corresponding author: Zou Juntao, Ph. D., Professor, Engineering Research Center of the Ministry of Education for Conductive Materials and Composite Technology, Xi'an University of Technology, Xi'an 710048, P. R. China, Tel: 0086-29-82312181, E-mail: zoujuntao@xaut.edu.cn

Copyright © 2022, Northwest Institute for Nonferrous Metal Research. Published by Science Press. All rights reserved.

1 Experiment

The blade of nickel-based DD483 superalloy was used as the raw materials and its chemical composition is listed in Table 1. The as-cast blade was firstly cut into small specimens by wire electrical discharge machining to avoid excessive stress. Then the specimens were sandblasted by quartz sand with 0.18 mm in diameter at pressure of 0.4~0.7 MPa for 30 s along the direction perpendicular to the surface and the distance of the spray gun was 100 mm away from the surface. These sandblasted specimens under different pressures were annealed in a tube furnace at 1100 °C for 4 and 16 h and then cooled down to room temperature inside the furnace. The whole annealing process was conducted in high pure argon atmosphere.

The residual stress on the surface of the sandblasted specimens was investigated by X-ray diffraction (XRD, D8-DISCOVERY). Laser scanning confocal microscope (OLS4000) was used to characterize the surface roughness. Microstructure observation was conducted by scanning electron microscope (SEM, JSM-6700F) and transmission electron microscope (TEM, JEM-3010). The components were analyzed by energy disperse spectroscopy (EDS). The specimens for SEM observation were treated through the standard grinding, and the mixture of 20 g CuSO₄, 100 mL HCl, and 100 mL H₂O was used for chemical etching. TEM specimens were prepared by a twin jet electro-polisher in a solution of 10vol% perchloric acid in ethanol at -30 °C and subsequently treated by ion milling operated at 4.5 kV with a tilting angle of ±5°.

2 Results and Discussion

2.1 Residual stress and surface roughness of DD483 superalloy after sandblasting

Fig. 1 shows the surface residual stress in DD483 alloy introduced by the sandblasting. All the negative values

Table 1 Composition of DD483 superalloy (wt%)

Cr	Co	Ti	W	Al	Ta	Mo	C	Ni
12.26	9.19	4.00	3.76	3.48	4.86	1.99	0.07	Bal.

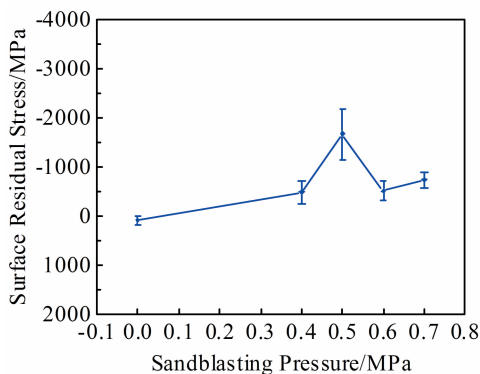


Fig. 1 Surface residual stress of DD483 superalloy under different sandblasting pressures

indicate that the compressive stress is already introduced by sandblasting. Another obvious feature is that there is a non-linear relationship between the surface stress and sandblasting pressure, which may be attributed to the unstable sandblasting pressure caused by the intermittent operation of air compressor during sandblasting. This problem is also commonly encountered in actual production. Therefore, it is necessary to measure the actual surface stress caused by sandblasting. The measured values in Fig. 1 can be used as a reference for the subsequent discussion.

The surface roughness R_a of sandblasted specimens under different sandblasting pressures is shown in Fig. 2. The surface roughness is obviously improved after sandblasting. In addition, the surface is flattened after sandblasting at pressure of 0.4 MPa. Subsequently, the surface roughness tends to be stable with increasing the pressure, because the sand particles already affect the substrate and cannot further grind the surface layer. Therefore, the impurities such as oxides on the surface of DD483 superalloy can be effectively eliminated under the pressure of 0.4~0.7 MPa to avoid harmful effects in later process.

2.2 Recrystallization behavior of DD483 superalloy after sandblasting and annealing

The residual stress introduced by sandblasting can provide a certain driving force for the microstructural instability such as recrystallization and precipitation of topologically close-packed (TCP) phases during the high-temperature service of DD483 superalloy^[12-14]. These microstructural transformations can significantly impair the mechanical properties of materials^[15,16]. Accordingly, it is necessary to carefully investigate the high temperature stability of the superalloys after heat treatments to provide a theoretical guidance for the selection of sandblasting parameters.

2.2.1 Volatilization of surface elements

Although the nickel-based superalloys possess excellent oxidation resistance, oxygen pollution caused by volatilization of elements with low melting points may also occur in the

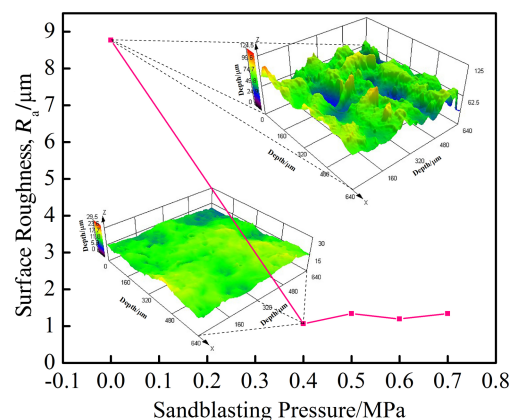


Fig. 2 Surface roughness R_a of DD483 superalloy under different sandblasting pressures

surface layer at high temperature^[17]. The surface element volatilization of the sandblasted specimens after annealing for 16 h is shown in Fig.3. Ti and Al elements volatilize to the surface, whereas the elements with high melting points, such as Ni, W, Co, and Ta, basically remain. After recrystallization, the surface oxide of Al and Ti produces a concentration gradient of Ni, W, and Ta elements by diffusion in recrystallization zone. Because Mo has the moderate antioxidant properties, compared with Ni, W, Ta, and Al, no concentration gradient of Mo is formed on the surface and inside of the alloy. So the dispersion distribution of Mo is stable, and plays an important role in matrix strengthening^[18]. Considering the EDS analysis in Fig.4, it can be concluded that a TiO₂ layer with the thickness of 8 μm is formed on the surface of DD483 superalloy, while a discontinuous Al₂O₃ layer with the thickness of about 7 μm is formed at the bottom of TiO₂ layer. Ti and Al elements can volatilize at high temperature and easily form related oxides on the surface layer. These titanium oxides tend to agglomerate into coarse particles, leaving a lot of cracks and providing the channel for oxygen diffusion into the substrate^[19]. The cracks can also be observed in Fig. 4. Therefore, the discontinuous aluminum oxides are generated by continuous internal oxidation at the cracks in substrate, and the growth of oxides promotes the crack expansion. In addition, a little Cr is gathered in the

surface layer in Fig.3, because the stress induced by sandblasting and subsequent thermal activation can promote the diffusion of Cr atoms to the interface between the substrate and the oxide layer^[20].

2.2.2 Microstructural evolution of surface layer

The surface microstructures of sandblasted specimens after annealing for 4 h are shown in Fig.5. After annealing for 4 h, the surface can be divided into three parts: oxide scale, recrystallization region, and original matrix. As shown in Fig. 5a, the surface oxide layer is mainly composed of TiO₂ and Al₂O₃. Single γ phase can be found at the bottom of the oxidation scales. The γ' phase disappears because the Al and Ti elements are consumed due to the oxidation behavior^[21]. Besides, the alloying elements such as W, Mo, and Ta can easily occupy the position of Al in the crystal structure of γ' phase. Consequently, the consumption of Al element also inhibits other solute atoms from entering the γ' phase. Meanwhile, the storage energy induced by sandblasting in the subsurface can also promote the dissolution of the γ' phase at high temperature. The single γ phase area can provide a favorable location of the nucleation for recrystallization behavior^[22], namely recrystallization region. Twins are formed in the region during the annealing process, as indicated by the arrow in Fig.5b. It is a normal phenomenon that strains can easily induce the grain boundary to form twin boundaries in

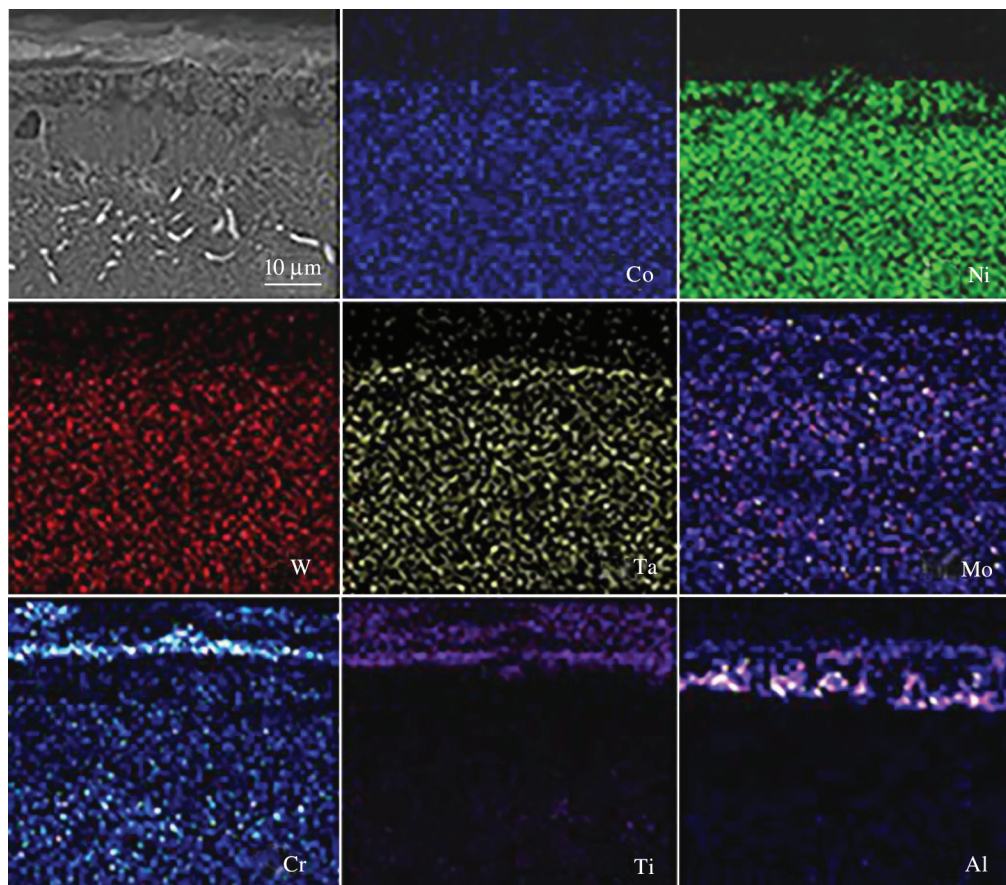


Fig.3 SEM image and corresponding EDS element mapping results of sandblasted specimen surface after annealing for 16 h

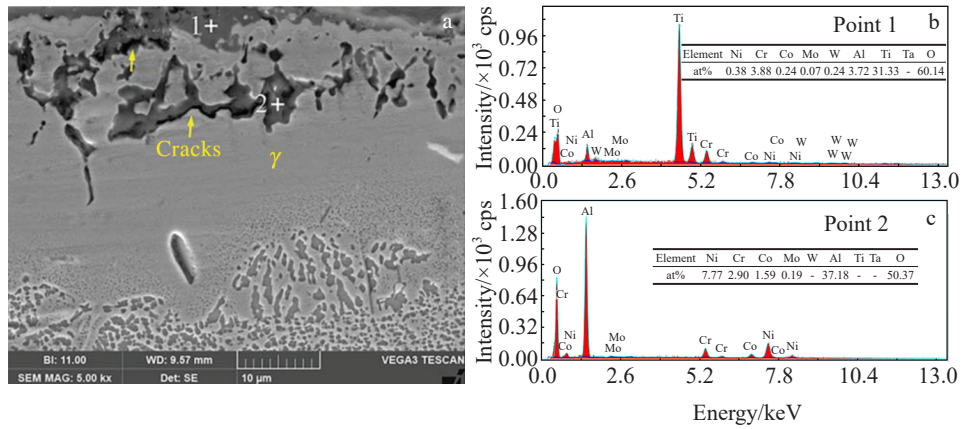


Fig.4 SEM image of sandblasted specimen surface after annealing for 16 h (a); EDS analysis results of point 1 (b) and point 2 (c) in Fig.4a

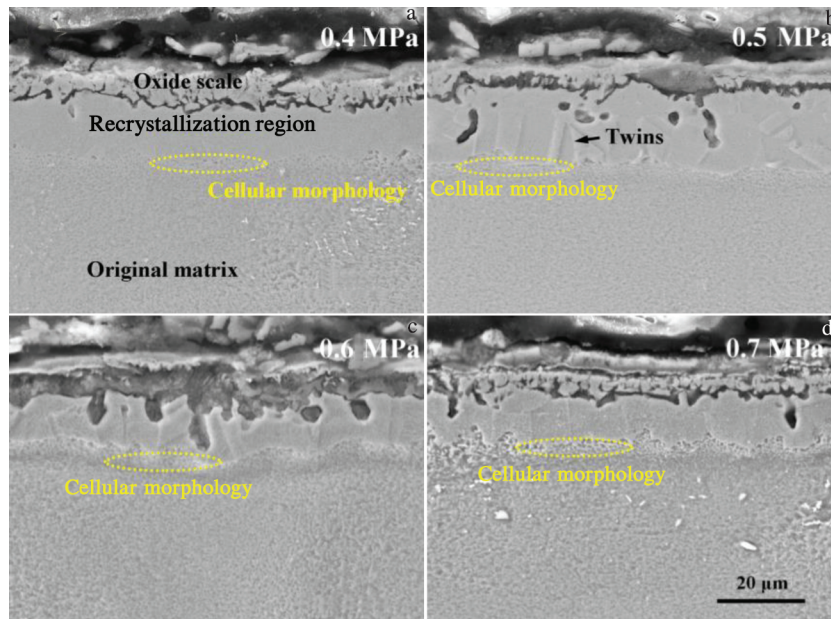


Fig.5 Microstructures of sandblasted specimen surface under different sandblasting pressures after annealing for 4 h: (a) 0.4 MPa, (b) 0.5 MPa, (c) 0.6 MPa, and (d) 0.7 MPa

superalloys with low stacking fault energy during recovery stage^[23]. A layer of cellular structure can be found in the recrystallization region, which suggests that recrystallization occurs, as indicated by the yellow dotted areas in Fig. 5. Actually, the cellular structure is the re-precipitated γ' phase during the recrystallization process. The above results are in good agreement with the reports of Zhang^[24] and Xiong^[25] et al. It is found that the cellular γ' phase can be obtained by the re-precipitation after dissolution of as-cast γ' phase in the early stage of recrystallization at the recrystallization region, and it can be later transformed into small and equiaxed γ' phase again. The formation of the cellular γ' phase is related to the solute saturation state caused by the dissolution of as-cast γ' phase. The supersaturated system with high energy will spontaneously change to the one with low energy by precipitation of discontinuous γ' phase with cellular

morphology^[25].

The surface microstructures of sandblasted specimens after annealing for 16 h are shown in Fig.6. Compared with that in the specimen annealed for 4 h, the internal oxidation of aluminum in specimen annealed for 16 h is more serious. Furthermore, the thickness of the cellular recrystallization layer of all the specimens annealed for 4 h is smaller than that annealed for 16 h, but no equiaxed crystals can be found in the annealed specimens. It can be concluded that a slight recrystallization occurs after annealing for 4 and 16 h at 1100 °C, but the recrystallization of specimens annealed for 16 h is more serious due to the longer holding time. There are some precipitates with granular and stripe morphologies in the recrystallization area^[26,27].

Fig. 7 shows the EDS results of the precipitations in recrystallization region and microstructural instability region.

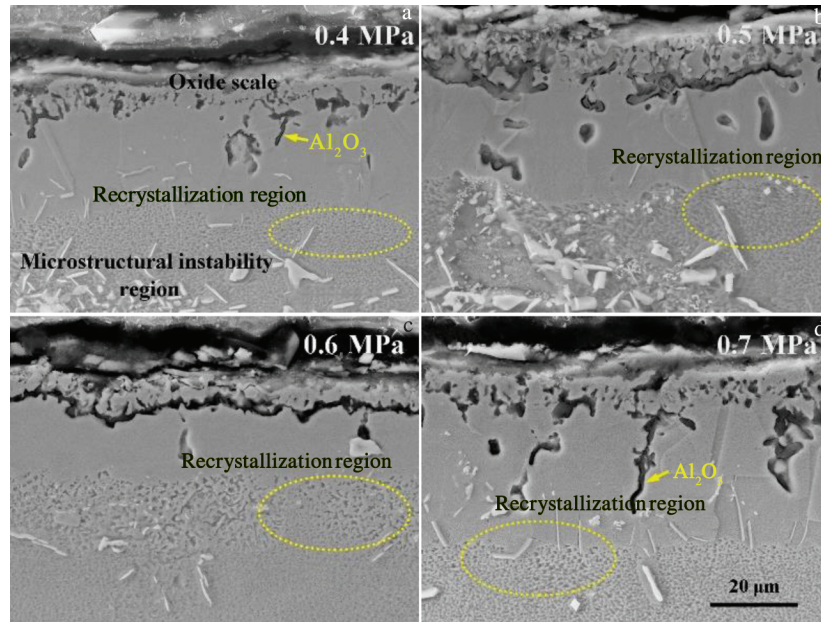


Fig.6 Microstructures of sandblasted specimen surface under different sandblasting pressures after annealing for 16 h: (a) 0.4 MPa, (b) 0.5 MPa, (c) 0.6 MPa, and (d) 0.7 MPa

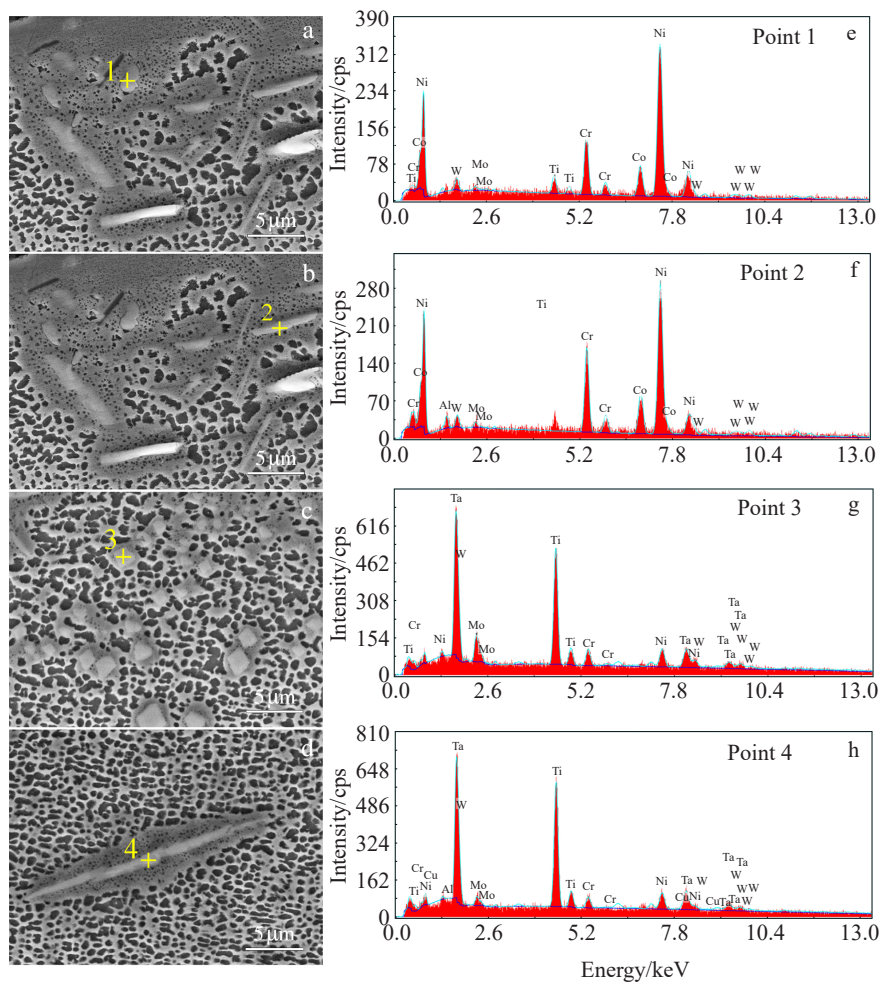


Fig.7 SEM images of precipitations in recrystallization region (a, b) and microstructural instability region (c, d); EDS spectra of point 1 in Fig.7a (e), point 2 in Fig.7b (f), point 3 in Fig.7c (g), and point 4 in Fig.7d (h)

From Fig. 7a and 7b, the components are considered as the TCP phase σ which possesses multiple morphologies, and the phase is further confirmed by TEM in Fig. 8. Zhuo et al.^[27] found that the instability of γ phase caused by the consumption of the surface Ni and Al elements promotes the precipitation of the TCP phase^[28]. Therefore, the formation of the TCP σ phase contributes to the interaction of element volatilization and redistribution. Precipitates are also found in the original matrix near the recrystallization region, namely microstructural instability region. The internal oxidation of aluminum is usually accompanied by the formation of TiN^[29]. Combining the EDS results in Fig. 7c and 7d with the selected area electron diffraction (SAED) analyses in Fig. 8, it can be inferred that TiN is generated. The granular and needle-shaped TiN in Fig. 7c and 7d was also determined by other researchers^[29]. However, because the titanium atoms in TiN can be easily replaced by tantalum atoms^[30], the tantalum content in the EDS spectra is high. The formation of internal oxides leads to the volume expansion, and some micro-cracks may be generated simultaneously to provide a path for the nitrogen to enter the original matrix.

The whole recrystallization region is harmful and its statistical depth collected in different locations as a function of sandblasting pressure is plotted in Fig. 9. The result shows that the whole recrystallization region of the specimens annealed for 16 h is deeper than that annealed for 4 h due to the longer holding time. In addition, the tendency of the depth of recrystallization region under different sandblasting pressures is similar to the variation of actual stress introduced by sandblasting. It suggests that the surface residual stress should be considered, which determines the depth of the

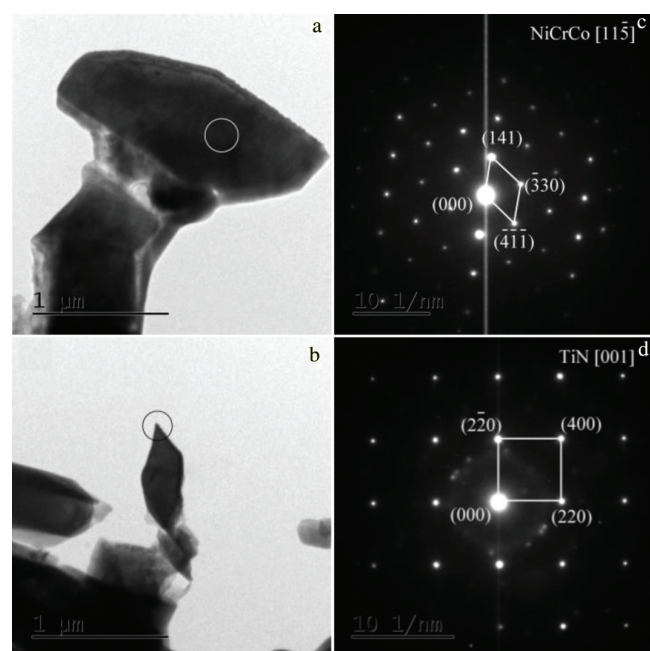


Fig. 8 TEM bright-field images (a, b) and SAED patterns (c, d) of TCP phase (a, c) and TiN (b, d)

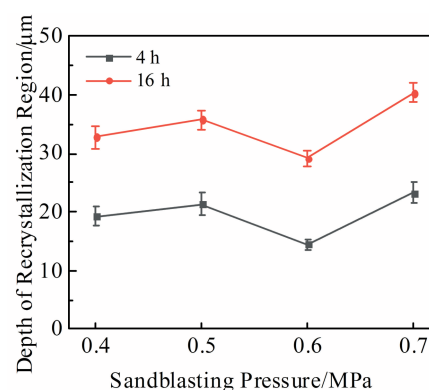


Fig. 9 Relationship between depth of recrystallization region and sandblasting pressure

recrystallization region.

3 Conclusions

1) Compressive stress is introduced into the surface of DD483 superalloy by sandblasting, and the surface can be cleaned at the sandblasting pressure of 0.4~0.7 MPa.

2) When the sandblasted specimens are annealed for 4 and 16 h, Ti and Al elements volatilize to the surface and are transformed into oxides. A small amount of Cr element diffuses to the surface due to the stress and thermal activation.

3) The cellular recrystallization structure appears in the recrystallization region of the sandblasted specimens annealed for 4 and 16 h. However, in the specimens annealed for 16 h, the cellular recrystallization structure is more and the topologically close-packed phase and TiN phase are precipitated in the recrystallization region and the original matrix near the recrystallization region, respectively.

4) The thickness of the recrystallization region is increased with increasing the annealing duration. The tendency of the depth of recrystallization region under different sandblasting pressures is similar to the variation of actual stress introduced by sandblasting.

References

- 1 Ma X F, Shi H J. *Int J Fatigue*[J], 2014, 61: 255
- 2 Li J, Wang H M. *Mater Sci Eng A*[J], 2010, 527: 4823
- 3 Zhang B, Lu X, Liu D L et al. *Mater Sci Eng A*[J], 2012, 551: 149
- 4 Meng J, Jin T, Sun X F et al. *Mater Sci Eng A*[J], 2010, 527: 6119
- 5 Xiong J C, Li J R, Liu S Z. *Chinese J Aeronaut*[J], 2010, 23(4): 478
- 6 Xu Z H, Huang G H, He L M et al. *J Alloy Compd*[J], 2014, 586: 1
- 7 Xie G, Zhang J, Lou L H et al. *Scripta Mater*[J], 2008, 59(8): 858
- 8 Wang L, Xie G, Zhang J et al. *Scripta Mater*[J], 2006, 55(5): 457
- 9 Zhang H B, Zhang K F, Jiang S S et al. *J Alloy Compd*[J], 2015,

- 623: 374
- 10 Zhuo L, Huang M, Wang F et al. *Mater Lett*[J], 2015, 139: 232
- 11 Xie G, Wang L, Zhang J et al. *Scripta Mater*[J], 2012, 66(6): 378
- 12 Mathur H, Panwisawas C, Jones C et al. *Acta Mater*[J], 2017, 129: 112
- 13 Rehman H, Durst K, Neumeier S et al. *Mater Sci Eng A*[J], 2015, 634: 202
- 14 Zhuo L C, Xiong J C, Chen Q Y et al. *Mater Sci Tech*[J], 2018, 34(6): 731
- 15 Sun W, Qin X Z, Guo J T et al. *Mater Des*[J], 2015, 69: 70
- 16 Qin X Z, Guo J T, Yuan C S et al. *Mater Sci Eng A*[J], 2012, 543: 121
- 17 Liu P S, Liang K M. *Oxid Met*[J], 2000, 53(3): 351
- 18 Wang D, Li Y S, Shi S J et al. *Mater Des*[J], 2020, 196: 109 077
- 19 Cao J D, Zhang J S, Chen R F et al. *Mater Charact*[J], 2016, 118: 122
- 20 Khan M A, Sundarajan S, Natarajan S et al. *Mater Manuf Processes*[J], 2014, 29(7): 832
- 21 Wang D, Li Y S, Shi S J et al. *Phil Mag Lett*[J], 2020, 100(5): 202
- 22 Mathur H, Panwisawas C, Jones C et al. *Acta Mater*[J], 2017, 129: 112
- 23 Bozzolo N, Souai N, Logé R et al. *Acta Mater*[J], 2012, 60: 5056
- 24 Zhang B, Cao X G, Liu D L et al. *T Nonferr Metal Soc*[J], 2013, 23(5): 1286
- 25 Xiong J C, Li J R, Liu S Z. *Chinese J Aeronaut*[J], 2010, 23(4): 478
- 26 Du J, Zhang J J, Wang L G et al. *Rare Metal Mat Eng*[J], 2018, 47(8): 2275
- 27 Zhuo L C, Huang M, Wang F et al. *Mater Lett*[J], 2015, 143: 305
- 28 Guruswamy S, Park S M, Hirth J P et al. *Oxid Met*[J], 1986, 26(1-2): 77
- 29 Pfennig A, Fedelich B. *Corros Sci*[J], 2008, 50(9): 2484
- 30 Ren W L, Ouyang F F, Ding B et al. *J Alloy Compd*[J], 2017, 724: 565

喷砂和退火对DD483合金表面再结晶的影响

邹军涛¹, 宋大拙¹, 雷 艺^{1,2}, 卓龙超¹, 商 昭¹, 杨功显², 张琼元², 巩秀芳²

(1. 西安理工大学 导电材料与复合技术教育部工程研究中心, 陕西 西安 710048)

(2. 东方汽轮机股份有限公司 长寿命高温材料国家重点实验室, 四川 德阳 618000)

摘 要: 研究了DD483合金在服役温度附近经喷砂处理和退火后的组织演变和表面再结晶行为。将DD483合金试样在0.4~0.7 MPa的压力范围内进行喷砂处理, 再于1100 ℃退火4和16 h。结果表明, 在预定的爆破压力范围内, 喷砂能有效地清理合金表面, 并将压应力引入表面。喷砂样品退火4和16 h后, Ti和Al元素析出到表面并转化为氧化物, 退火后亚表层出现胞状再结晶结构。拓扑密堆积(TCP)相和TiN分别在再结晶区和原始基体近再结晶区析出。此外, 再结晶区的厚度随退火时间和实际应力的增加而增加。

关键词: 镍基高温合金; 喷砂; 退火; 再结晶; 表面; 微观结构

作者简介: 邹军涛, 男, 1979年生, 博士, 教授, 西安理工大学导电材料与复合技术教育部工程研究中心, 陕西 西安 710048, 电话: 029-82312181, E-mail: zoujuntao@xaut.edu.cn